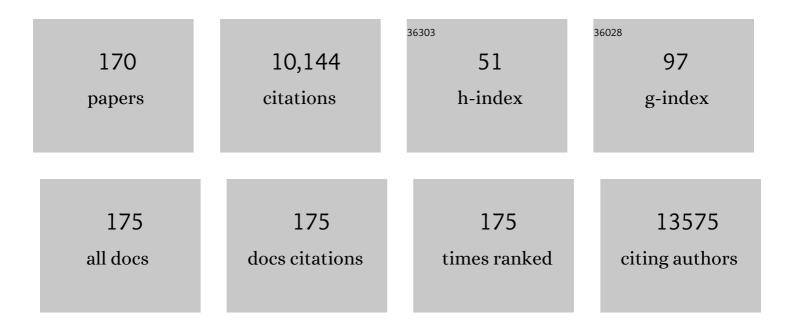
## Jefferson Zhe Liu

List of Publications by Year in descending order

Source: https://exaly.com/author-pdf/4924950/publications.pdf Version: 2024-02-01



#	Article	IF	CITATIONS
1	Detecting subtle yet fast skeletal muscle contractions with ultrasoft and durable graphene-based cellular materials. National Science Review, 2022, 9, nwab184.	9.5	4
2	Ferromagnetic and nonmagnetic <mml:math xmlns:mml="http://www.w3.org/1998/Math/MathML"&gt;<mml:mrow><mml:mn>1</mml:mn><mml:msup><mml charge density wave states in transition metal dichalcogenides: Physical mechanisms and charge doping induced reversible transition. Physical Review B, 2022, 105, .</mml </mml:msup></mml:mrow></mml:math 	:mi>T3.2	nl:mj> <mml:n< td=""></mml:n<>
3	Van der Waals force-induced intralayer ferroelectric-to-antiferroelectric transition via interlayer sliding in bilayer group-IV monochalcogenides. Npj Computational Materials, 2022, 8, .	8.7	20
4	The interfacial adhesion of contacting pairs in van der Waals materials. Applied Surface Science, 2022, 598, 153739.	6.1	3
5	Quadrupling the stored charge by extending the accessible density of states. CheM, 2022, 8, 2410-2418.	11.7	4
6	Silica-assisted pyro-hydrolysis of CaCl2 waste for the recovery of hydrochloric acid (HCl): Reaction pathways with the evolution of Ca(OH)Cl intermediate by experimental investigation and DFT modelling. Journal of Hazardous Materials, 2022, 439, 129620.	12.4	7
7	Ultrafast water evaporation through graphene membranes with subnanometer pores for desalination. Journal of Membrane Science, 2021, 621, 118934.	8.2	45
8	Diverse electronic and magnetic properties of CrS2 enabling strain-controlled 2D lateral heterostructure spintronic devices. Npj Computational Materials, 2021, 7, .	8.7	35
9	Direct identification of HMX via guest-induced fluorescence turn-on of molecular cage. Chinese Chemical Letters, 2021, 32, 4006-4010.	9.0	9
10	Nitrogen Rejection from Methane via a "Trapdoor―K-ZSM-25 Zeolite. Journal of the American Chemical Society, 2021, 143, 15195-15204.	13.7	19
11	Solvationâ€Involved Nanoionics: New Opportunities from 2D Nanomaterial Laminar Membranes. Advanced Materials, 2020, 32, e1904562.	21.0	61
12	Intrinsic Chirality and Multispectral Spinâ€Selective Transmission in Folded Etaâ€Shaped Metamaterials. Advanced Optical Materials, 2020, 8, 1901448.	7.3	36
13	Ab initio prediction of phase stability of martensitic structures in binary NiTi under hydrostatic tension. Physica Scripta, 2020, 95, 035701.	2.5	2
14	Rapid Bending Origami in Micro/Nanoscale toward a Versatile 3D Metasurface. Laser and Photonics Reviews, 2020, 14, 1900179.	8.7	12
15	Can CO <sub>2</sub> and Steam React in the Absence of Electrolysis at High Temperatures?. ChemSusChem, 2020, 13, 6660-6667.	6.8	4
16	Charge doping induced reversible multistep structural phase transitions and electromechanical actuation in two-dimensional 1T′-MoS <sub>2</sub> . Nanoscale, 2020, 12, 12541-12550.	5.6	19
17	Electrolyte gating in graphene-based supercapacitors and its use for probing nanoconfined charging dynamics. Nature Nanotechnology, 2020, 15, 683-689.	31.5	66
18	Thermodynamic, Structural, and Piezoelectric Properties of Adatom-Doped Phosphorene and Its Applications in Smart Surfaces. Physical Review Applied, 2020, 13, .	3.8	4

#	Article	IF	CITATIONS
19	Lead-free molecular ferroelectric [N,N-dimethylimidazole]3Bi2I9 with narrow bandgap. Materials and Design, 2020, 193, 108868.	7.0	8
20	Efficient metal ion sieving in rectifying subnanochannels enabled by metal–organic frameworks. Nature Materials, 2020, 19, 767-774.	27.5	275
21	Universal Approach to Fabricating Graphene-Supported Single-Atom Catalysts from Doped ZnO Solid Solutions. ACS Central Science, 2020, 6, 1431-1440.	11.3	69
22	The Role of Nanowrinkles in Mass Transport across Grapheneâ€Based Membranes. Advanced Functional Materials, 2020, 30, 2003159.	14.9	39
23	Circular Dichroism: Intrinsic Chirality and Multispectral Spinâ€Selective Transmission in Folded Etaâ€Shaped Metamaterials (Advanced Optical Materials 4/2020). Advanced Optical Materials, 2020, 8, 2070014.	7.3	1
24	Risk assessment through multivariate analysis on the magnitude and occurrence date of daily storm events in the Shenzhen bay area. Stochastic Environmental Research and Risk Assessment, 2020, 34, 669-689.	4.0	5
25	Separation of CO <sub>2</sub> and CH <sub>4</sub> by Pressure Swing Adsorption Using a Molecular Trapdoor Chabazite Adsorbent for Natural Gas Purification. Industrial & Engineering Chemistry Research, 2020, 59, 7857-7865.	3.7	44
26	Monoclinic angle, shear response, and minimum energy pathways of NiTiCu martensite phases from ab initio calculations. Acta Materialia, 2019, 178, 59-67.	7.9	4
27	Ultrafast, Stable Ionic and Molecular Sieving through Functionalized Boron Nitride Membranes. ACS Applied Materials & Interfaces, 2019, 11, 30430-30436.	8.0	25
28	Revealing Atomic Structure and Oxidation States of Dopants in Charge-Ordered Nanoparticles for Migration-Promoted Oxygen-Exchange Capacity. Chemistry of Materials, 2019, 31, 5769-5777.	6.7	10
29	3D Micro/Nano Structures: Folding 2D Structures into 3D Configurations at the Micro/Nanoscale: Principles, Techniques, and Applications (Adv. Mater. 4/2019). Advanced Materials, 2019, 31, 1970025.	21.0	1
30	Fast and selective fluoride ion conduction in sub-1-nanometer metal-organic framework channels. Nature Communications, 2019, 10, 2490.	12.8	158
31	Broadband and Polarization-Insensitive Absorption Based on a Set of Multisized Fabry–Perot-like Resonators. Journal of Physical Chemistry C, 2019, 123, 13856-13862.	3.1	24
32	Computational Design of Functionally Graded Materials from Sintered Powders. Integrating Materials and Manufacturing Innovation, 2019, 8, 82-94.	2.6	4
33	A Raman spectroscopy study of MBE-grown Hg1â^'Cd Se alloys grown on GaSb (2 1 1) by molecular beam epitaxy. Infrared Physics and Technology, 2019, 97, 365-370.	2.9	9
34	Tuning capacitance of graphene films via a robust routine of adjusting their hierarchical structures. Electrochimica Acta, 2019, 298, 254-264.	5.2	14
35	Spin-Selective Transmission in Chiral Folded Metasurfaces. Nano Letters, 2019, 19, 3432-3439.	9.1	89
36	Folding 2D Structures into 3D Configurations at the Micro/Nanoscale: Principles, Techniques, and Applications. Advanced Materials, 2019, 31, e1802211.	21.0	39

k

#	Article	IF	CITATIONS
37	Density functional theory computational study of ferroelectricity and piezoelectricity in BaTiO <sub>3</sub> /PbTiO <sub>3</sub> (0 1 1) superlattices. Journal of Physics Condensed Matter, 202 30, 155401.	18,,8	1
38	Role of hydrostatic pressure on the phase stability, the ground state, and the transformation pathways of NiTi alloy. Scripta Materialia, 2018, 151, 57-60.	5.2	14
39	Finite element models of natural fibers and their composites: A review. Journal of Reinforced Plastics and Composites, 2018, 37, 617-635.	3.1	58
40	Ultrafast selective transport of alkali metal ions in metal organic frameworks with subnanometer pores. Science Advances, 2018, 4, eaaq0066.	10.3	368
41	An equivalent 1D nanochannel model to describe ion transport in multilayered graphene membranes. Progress in Natural Science: Materials International, 2018, 28, 246-250.	4.4	9
42	Ferromagnetism of 1T′-MoS <sub>2</sub> Nanoribbons Stabilized by Edge Reconstruction and Its Periodic Variation on Nanoribbons Width. Journal of the American Chemical Society, 2018, 140, 16206-16212.	13.7	39
43	Tunable auxetic properties in group-IV monochalcogenide monolayers. Physical Review B, 2018, 98, .	3.2	42
44	Tunable near-infrared perfect absorber based on the hybridization of phase-change material and nanocross-shaped resonators. Applied Physics Letters, 2018, 113, .	3.3	27
45	Low-voltage electrostatic modulation of ion diffusion through layered graphene-based nanoporous membranes. Nature Nanotechnology, 2018, 13, 685-690.	31.5	196
46	An ICME Framework for Design of Stainless Steel for Sintering. Integrating Materials and Manufacturing Innovation, 2018, 7, 136-147.	2.6	4
47	Room temperature in-plane ferroelectricity in van der Waals In <sub>2</sub> Se <sub>3</sub> . Science Advances, 2018, 4, eaar7720.	10.3	224
48	Design and commissioning of an aberration-corrected ultrafast spin-polarized low energy electron microscope with multiple electron sources. Ultramicroscopy, 2017, 174, 89-96.	1.9	10
49	<i>Ab Initio</i> Simulations To Understand the Leaf-Shape Crystal Morphology of ZIF-L with Two-Dimensional Layered Network. Journal of Physical Chemistry C, 2017, 121, 2221-2227.	3.1	35
50	Highâ€Qualityâ€Factor Midâ€Infrared Toroidal Excitation in Folded 3D Metamaterials. Advanced Materials, 2017, 29, 1606298.	21.0	117
51	Negative Poisson's ratio in rippled graphene. Nanoscale, 2017, 9, 4135-4142.	5.6	70
52	Metamaterials: Highâ€Qualityâ€Factor Midâ€Infrared Toroidal Excitation in Folded 3D Metamaterials (Adv.) Tj ETC	2 <u>99</u> 80 rş	gBT /Overloo
53	Integrating polarization conversion and nearly perfect absorption with multifunctional metasurfaces. Applied Physics Letters, 2017, 110, .	3.3	49

54Field-Effect Tuned Adsorption Dynamics of VSe<sub>2</sub> Nanosheets for Enhanced Hydrogen9.113454Evolution Reaction. Nano Letters, 2017, 17, 4109-4115.9.1134

#	Article	IF	CITATIONS
55	Temperature-regulated guest admission and release in microporous materials. Nature Communications, 2017, 8, 15777.	12.8	60
56	Evaluation of Textural Effect on the Rollability of AZ31 Alloys by Wedge‧haped Sample Design. Advanced Engineering Materials, 2017, 19, 1700035.	3.5	2
57	Fano resonance Rabi splitting of surface plasmons. Scientific Reports, 2017, 7, 8010.	3.3	57
58	Oxygen evolution reaction dynamics monitored by an individual nanosheet-based electronic circuit. Nature Communications, 2017, 8, 645.	12.8	49
59	Extremely Low Density and Superâ€Compressible Graphene Cellular Materials. Advanced Materials, 2017, 29, 1701553.	21.0	126
60	Tailoring the Microstructure and Mechanical Property of AZ80 Alloys by Multiple Twinning and Aging Precipitation. Advanced Engineering Materials, 2017, 19, 1700332.	3.5	10
61	Evaluation of support loss in micro-beam resonators: A revisit. Journal of Sound and Vibration, 2017, 411, 148-164.	3.9	9
62	A density functional theory computational study of adsorption of Di-Meta-Cyano Azobenzene molecules on Si (111) surfaces. Applied Surface Science, 2017, 422, 557-565.	6.1	7
63	Enhanced in-plane mechanical properties of nanoporous graphene-carbon nanotube network. Journal of Applied Physics, 2017, 121, .	2.5	6
64	Broadband cross-polarization conversion by symmetry-breaking ultrathin metasurfaces. Applied Physics Letters, 2017, 111, 241108.	3.3	20
65	Reply to 'On phonons and water flow enhancement in carbon nanotubes'. Nature Nanotechnology, 2017, 12, 1108-1108.	31.5	0
66	Controllable optical activity with non-chiral plasmonic metasurfaces. Light: Science and Applications, 2016, 5, e16096-e16096.	16.6	70
67	Comparative study on twinning characteristics during two post-weld compression paths and their effects on joint enhancement. Scientific Reports, 2016, 6, 39779.	3.3	13
68	Fabrication of GaN hexagonal cones by inductively coupled plasma reactive ion etching. Journal of Vacuum Science and Technology B:Nanotechnology and Microelectronics, 2016, 34, .	1.2	10
69	Spatially oriented plasmonic †nanograter' structures. Scientific Reports, 2016, 6, 28764.	3.3	12
70	Two-way actuation of graphene oxide arising from quantum mechanical effects. Applied Physics Letters, 2016, 109, 143902.	3.3	4
71	Electric Field Induced Reversible Phase Transition in Li Doped Phosphorene: Shape Memory Effect and Superelasticity. Journal of the American Chemical Society, 2016, 138, 4772-4778.	13.7	26
72	Sustaining GHz oscillation of carbon nanotube based oscillators via a MHz frequency excitation. Nanotechnology, 2016, 27, 205501.	2.6	3

#	Article	IF	CITATIONS
73	Light emitting enhancement and angle-resolved property of surface textured GaN-based vertical LED. Journal of Optics (India), 2016, 45, 81-86.	1.7	8
74	Asymmetrically porous anion exchange membranes with an ultrathin selective layer for rapid acid recovery. Journal of Membrane Science, 2016, 510, 437-446.	8.2	27
75	Mechanical properties of wrinkled graphene generated by topological defects. Carbon, 2016, 108, 204-214.	10.3	72
76	Mass Production of Nanogap Electrodes toward Robust Resistive Random Access Memory. Advanced Materials, 2016, 28, 8227-8233.	21.0	20
77	Excitation of ultrasharp trapped-mode resonances in mirror-symmetric metamaterials. Physical Review B, 2016, 93, .	3.2	39
78	Strain Relaxation of Monolayer WS <sub>2</sub> on Plastic Substrate. Advanced Functional Materials, 2016, 26, 8707-8714.	14.9	97
79	3D conductive coupling for efficient generation of prominent Fano resonances in metamaterials. Scientific Reports, 2016, 6, 27817.	3.3	43
80	Two-dimensional shape memory graphene oxide. Nature Communications, 2016, 7, 11972.	12.8	33
81	A density functional theory study for the adsorption of various gases on a caesium-exchanged trapdoor chabazite. Computational Materials Science, 2016, 122, 307-313.	3.0	25
82	Molecular dynamics simulations of the electric double layer capacitance of graphene electrodes in mono-valent aqueous electrolytes. Nano Research, 2016, 9, 174-186.	10.4	77
83	Ultrafast Dynamic Piezoresistive Response of Grapheneâ€Based Cellular Elastomers. Advanced Materials, 2016, 28, 194-200.	21.0	171
84	lon transport in complex layered graphene-based membranes with tuneable interlayer spacing. Science Advances, 2016, 2, e1501272.	10.3	203
85	Aqueous Phase Synthesis of ZIF-8 Membrane with Controllable Location on an Asymmetrically Porous Polymer Substrate. ACS Applied Materials & Interfaces, 2016, 8, 6236-6244.	8.0	95
86	Porous diffusion dialysis membranes for rapid acid recovery. Journal of Membrane Science, 2016, 502, 76-83.	8.2	52
87	Anomalous elastic buckling of layered crystalline materials in the absence of structure slenderness. Journal of the Mechanics and Physics of Solids, 2016, 88, 83-99.	4.8	24
88	Mechanical buckling induced periodic kinking/stripe microstructures in mechanically peeled graphite flakes from HOPG. Acta Mechanica Sinica/Lixue Xuebao, 2015, 31, 494-499.	3.4	4
89	Tunable mid-infrared coherent perfect absorption in a graphene meta-surface. Scientific Reports, 2015, 5, 13956.	3.3	115
90	Three Dimensional Hybrids of Vertical Graphene-nanosheet Sandwiched by Ag-nanoparticles for Enhanced Surface Selectively Catalytic Reactions. Scientific Reports, 2015, 5, 16019.	3.3	59

#	Article	IF	CITATIONS
91	Directly patterned substrate-free plasmonic "nanograter―structures with unusual Fano resonances. Light: Science and Applications, 2015, 4, e308-e308.	16.6	105
92	Highâ€Performance Broadband Circularly Polarized Beam Deflector by Mirror Effect of Multinanorod Metasurfaces. Advanced Functional Materials, 2015, 25, 5428-5434.	14.9	69
93	Metal–Organic Polyhedra Cages Immobilized on a Plasmonic Substrate for Sensitive Detection of Trace Explosives. Advanced Functional Materials, 2015, 25, 6009-6017.	14.9	47
94	Beam Deflectors: Highâ€Performance Broadband Circularly Polarized Beam Deflector by Mirror Effect of Multinanorod Metasurfaces (Adv. Funct. Mater. 34/2015). Advanced Functional Materials, 2015, 25, 5567-5567.	14.9	0
95	Rapid synthesis of ultrathin, defect-free ZIF-8 membranes via chemical vapour modification of a polymeric support. Chemical Communications, 2015, 51, 11474-11477.	4.1	103
96	Fabrication of asymmetrical diffusion dialysis membranes for rapid acid recovery with high purity. Journal of Materials Chemistry A, 2015, 3, 24000-24007.	10.3	49
97	Thermal induced single grain boundary break junction for suspended nanogap electrodes. Science China Materials, 2015, 58, 769-774.	6.3	4
98	The concept and realization of nanostructure fabrication using free-standing metallic wires with rapid thermal annealing. Science China: Physics, Mechanics and Astronomy, 2015, 58, 1-7.	5.1	1
99	Cation ordering induced polarization enhancement for <mml:math xmlns:mml="http://www.w3.org/1998/Math/MathML"&gt;<mml:msub><mml:mi>PbTiO</mml:mi><mml:mn>3superlattices. Physical Review B, 2015, 91, .</mml:mn></mml:msub></mml:math 	າ <b>l:nສມ2</b> > <td>.m<b>k</b>msub&gt;<m< td=""></m<></td>	.m <b>k</b> msub> <m< td=""></m<>
100	Water transport inside carbon nanotubes mediated by phonon-induced oscillating friction. Nature Nanotechnology, 2015, 10, 692-695.	31.5	142
101	Oriented two-dimensional zeolitic imidazolate framework-L membranes and their gas permeation properties. Journal of Materials Chemistry A, 2015, 3, 15715-15722.	10.3	149
102	Cooperative Reformable Channel System with Unique Recognition of Gas Molecules in a Zeolitic Imidazolate Framework with Multilevel Flexible Ligands. Journal of Physical Chemistry C, 2015, 119, 16762-16768.	3.1	9
103	Single Grain Boundary Break Junction for Suspended Nanogap Electrodes with Gapwidth Down to 1–2 nm by Focused Ion Beam Milling. Advanced Materials, 2015, 27, 3002-3006.	21.0	59
104	Nanogap Electrodes: Single Grain Boundary Break Junction for Suspended Nanogap Electrodes with Gapwidth Down to 1–2 nm by Focused Ion Beam Milling (Adv. Mater. 19/2015). Advanced Materials, 2015, 27, 3095-3095.	21.0	4
105	Composite ultrafiltration membranes from polymer and its quaternary phosphonium-functionalized derivative with enhanced water flux. Journal of Membrane Science, 2015, 482, 67-75.	8.2	44
106	Polysulfone and Its Quaternary Phosphonium Derivative Composite Membranes with High Water Flux. Industrial & Engineering Chemistry Research, 2015, 54, 3333-3340.	3.7	11
107	The activation of twinning and texture evolution during bending of friction stir welded magnesium alloys. Materials Science & Engineering A: Structural Materials: Properties, Microstructure and Processing, 2015, 646, 145-153.	5.6	30
108	Tuning the oxygen functional groups in reduced graphene oxide papers to enhance the electromechanical actuation. RSC Advances, 2015, 5, 68052-68060.	3.6	9

#	Article	IF	CITATIONS
109	Density Functional Theory Computational Study of Alkali Cation-Exchanged Sodalite-like Zeolitelike Metal–Organic Framework for CO2, N2, and CH4 Adsorption. Journal of Physical Chemistry C, 2015, 119, 27449-27456.	3.1	7
110	Adsorption of CO2, N2, and CH4 in Cs-exchanged chabazite: A combination of van der Waals density functional theory calculations and experiment study. Journal of Chemical Physics, 2014, 140, 084705.	3.0	43
111	Brownian motion-induced water slip inside carbon nanotubes. Microfluidics and Nanofluidics, 2014, 16, 305-313.	2.2	4
112	Plasmonic Coupling: Wafer-Scale Double-Layer Stacked Au/Al2O3@Au Nanosphere Structure with Tunable Nanospacing for Surface-Enhanced Raman Scattering (Small 19/2014). Small, 2014, 10, 3932-3932.	10.0	2
113	Hydrophilic Nanowire Modified Polymer Ultrafiltration Membranes with High Water Flux. ACS Applied Materials & Interfaces, 2014, 6, 19161-19167.	8.0	22
114	Temperature controlled invertible selectivity for adsorption of N2 and CH4 by molecular trapdoor chabazites. Chemical Communications, 2014, 50, 4544.	4.1	33
115	Slow hydrophobic hydration induced polymer ultrafiltration membranes with high water flux. Journal of Membrane Science, 2014, 471, 27-34.	8.2	32
116	Enhanced light extraction in n-GaN-based light-emitting diodes with three-dimensional semi-spherical structure. Applied Physics Letters, 2014, 104, .	3.3	11
117	Piezoelectric properties of graphene oxide: A first-principles computational study. Applied Physics Letters, 2014, 105, .	3.3	58
118	Comparison of continuum-based and atomistic-based modeling of axial buckling of carbon nanotubes subject to hydrostatic pressure. Computational Materials Science, 2013, 79, 619-626.	3.0	13
119	Enhanced lithium adsorption and diffusion on silicene nanoribbons. RSC Advances, 2013, 3, 20338.	3.6	26
120	Control of surface wettability via strain engineering. Acta Mechanica Sinica/Lixue Xuebao, 2013, 29, 543-549.	3.4	19
121	Determination of Composition Range for "Molecular Trapdoor―Effect in Chabazite Zeolite. Journal of Physical Chemistry C, 2013, 117, 12841-12847.	3.1	104
122	A simulation study of the shape of β′ precipitates in Mg–Y and Mg–Gd alloys. Acta Materialia, 2013, 61, 453-466.	7.9	150
123	Periodic Segregation of Solute Atoms in Fully Coherent Twin Boundaries. Science, 2013, 340, 957-960.	12.6	659
124	Fabrication of indium tin oxide bump/pit structures on GaN-based light emitting diodes. Journal of Vacuum Science and Technology B:Nanotechnology and Microelectronics, 2013, 31, .	1.2	0
125	Ion-beam-induced bending of freestanding amorphous nanowires: The importance of the substrate material and charging. Applied Physics Letters, 2013, 102, .	3.3	22
126	Binding and interlayer force in the near-contact region of two graphite slabs: Experiment and theory. Journal of Chemical Physics, 2013, 139, 224704.	3.0	21

#	Article	IF	CITATIONS
127	Monolayer graphene oxide as a building block for artificial muscles. Applied Physics Letters, 2013, 102, 021903.	3.3	26
128	Tuning the oscillation of nested carbon nanotubes by insertion of an additional inner tube. Journal of Applied Physics, 2013, 114, 214302.	2.5	7
129	Graphene Electromechanical Actuation; Origins, Optimization and Applications. Materials Research Society Symposia Proceedings, 2012, 1407, 39.	0.1	Ο
130	Sensing properties of infrared nanostructured plasmonic crystals fabricated by electron beam lithography and argon ion milling. Journal of Vacuum Science and Technology B:Nanotechnology and Microelectronics, 2012, 30, 06FE02.	1.2	1
131	Freestanding nanostructures for three-dimensional superconducting nanodevices. Applied Physics Letters, 2012, 100, .	3.3	18
132	Observation of Microscale Superlubricity in Graphite. Physical Review Letters, 2012, 108, 205503.	7.8	431
133	Discriminative Separation of Gases by a "Molecular Trapdoor―Mechanism in Chabazite Zeolites. Journal of the American Chemical Society, 2012, 134, 19246-19253.	13.7	321
134	Biomimetic superelastic graphene-based cellular monoliths. Nature Communications, 2012, 3, 1241.	12.8	1,091
135	Visible transmission response of nanoscale complementary metamaterials for sensing applications. Nanotechnology, 2012, 23, 275503.	2.6	12
136	Interlayer shear strength of single crystalline graphite. Acta Mechanica Sinica/Lixue Xuebao, 2012, 28, 978-982.	3.4	86
137	Influence of Electric Field on SERS: Frequency Effects, Intensity Changes, and Susceptible Bonds. Journal of the American Chemical Society, 2012, 134, 4646-4653.	13.7	41
138	Band engineering of Ni1â^'xMgxO alloys for photocathodes of high efficiency dye-sensitized solar cells. Journal of Applied Physics, 2012, 112, .	2.5	27
139	Interlayer binding energy of graphite: A mesoscopic determination from deformation. Physical Review B, 2012, 85, .	3.2	203
140	Phase inversion spinning of ultrafine hollow fiber membranes through a single orifice spinneret. Journal of Membrane Science, 2012, 421-422, 8-14.	8.2	23
141	High-Performance Graphene Oxide Electromechanical Actuators. Journal of the American Chemical Society, 2012, 134, 1250-1255.	13.7	44
142	Edge stresses of non-stoichiometric edges in two-dimensional crystals. Applied Physics Letters, 2012, 100, .	3.3	21
143	Graphite flake self-retraction response based on potential seeking. Nanoscale Research Letters, 2012, 7, 185.	5.7	9
144	Graphene Actuators: Quantum-Mechanical and Electrostatic Double-Layer Effects. Journal of the American Chemical Society, 2011, 133, 10858-10863.	13.7	101

#	Article	IF	CITATIONS
145	Nanoscale fluid-structure interaction: Flow resistance and energy transfer between water and carbon nanotubes. Physical Review E, 2011, 84, 046314.	2.1	36
146	Strain engineering water transport in graphene nanochannels. Physical Review E, 2011, 84, 056329.	2.1	101
147	Viscous damping of nanobeam resonators: Humidity, thermal noise, and a paddling effect. Journal of Applied Physics, 2011, 110, .	2.5	21
148	Friction of water slipping in carbon nanotubes. Physical Review E, 2011, 83, 036316.	2.1	80
149	Influence of Parameters of Cold Isostatic Pressing on TiO <sub>2</sub> Films for Flexible Dye-Sensitized Solar Cells. International Journal of Photoenergy, 2011, 2011, 1-7.	2.5	14
150	Effects of vacancies on interwall spacings of multi-walled carbon nanotubes. Journal of Zhejiang University: Science A, 2010, 11, 714-721.	2.4	2
151	Bridging the gap between atomic microstructure and electronic properties of alloys: The case of (In,Ga)N. Physical Review B, 2010, 82, .	3.2	39
152	Stripe/kink microstructures formed in mechanical peeling of highly orientated pyrolytic graphite. Applied Physics Letters, 2010, 96, .	3.3	19
153	Reversible high-pressure carbon nanotube vessel. Physical Review B, 2010, 81, .	3.2	7
154	Potassium Chabazite: A Potential Nanocontainer for Gas Encapsulation. Journal of Physical Chemistry C, 2010, 114, 22025-22031.	3.1	45
155	Friction law for water flowing in carbon nanotubes. , 2010, , .		3
156	Prediction of ordering and spontaneous rotation of epitaxial habits in substrate-coherent InGaN and GaAsSb. Applied Physics Letters, 2009, 95, 081901.	3.3	3
157	Tunable resonant frequencies for determining Young's moduli of nanowires. Journal of Applied Physics, 2009, 105, .	2.5	10
158	Thermodynamic theory of epitaxial alloys: first-principles mixed-basis cluster expansion of (In, Ga)N alloy film. Journal of Physics Condensed Matter, 2009, 21, 295402.	1.8	13
159	Thermodynamic states and phase diagrams for bulk-incoherent, bulk-coherent, and epitaxially-coherent semiconductor alloys: Application to cubic (Ga,In)N. Physical Review B, 2008, 77, .	3.2	62
160	Relative stability, electronic structure, and magnetism of MnN and (Ga,Mn)N alloys. Physical Review B, 2008, 78, .	3.2	39
161	Fast Liquid Jet Mixing in Millimeter Channels with Various Multislits Designs. Industrial & Engineering Chemistry Research, 2008, 47, 9744-9753.	3.7	10
162	Strain-Minimizing Tetrahedral Networks of Semiconductor Alloys. Physical Review Letters, 2007, 99, 145501.	7.8	26

#	Article	IF	CITATIONS
163	Transferable force-constant modeling of vibrational thermodynamic properties in fcc-basedAlâ^'TM(TM=Ti, Zr, Hf) alloys. Physical Review B, 2007, 75, .	3.2	44
164	An unsolved mystery: The composition of bcc Cu alloy precipitates in bcc Fe and steels. Materials Science & Engineering A: Structural Materials: Properties, Microstructure and Processing, 2007, 463, 271-274.	5.6	77
165	Mechanical properties of single-walled carbon nanotube bundles as bulk materials. Journal of the Mechanics and Physics of Solids, 2005, 53, 123-142.	4.8	80
166	Size Dependence of the Thin-Shell Model for Carbon Nanotubes. Physical Review Letters, 2005, 95, 105501.	7.8	157
167	Structure, energetics, and mechanical stability of Fe-Cu bcc alloys from first-principles calculations. Physical Review B, 2005, 72, .	3.2	120
168	Effect of bending instabilities on the measurements of mechanical properties of multiwalled carbon nanotubes. Physical Review B, 2003, 67, .	3.2	48
169	Excess van der Waals interaction energy of a multiwalled carbon nanotube with an extruded core and the induced core oscillation. Physical Review B, 2002, 65, .	3.2	220
170	Effect of a Rippling Mode on Resonances of Carbon Nanotubes. Physical Review Letters, 2001, 86, 4843-4846.	7.8	120